Nuclear Spin Relaxation in Alkali Metals*

D. F. Holcomb† AND R. E. Norberg‡

Department of Physics, University of Illinois, Urbana, Illinois

(Received September 23, 1954)

Nuclear magnetic resonance measurements have been made in metallic lithium, sodium, and rubidium, using pulsed radio-frequency power. The experimental data are values of T_1, the spin-lattice relaxation time, and of T_2, the inverse line width or spin-spin relaxation time. Measurements were made at several Larmor frequencies and at temperatures between $-65°C$ and $250°C$. Over a considerable temperature range, T_1 is found to be primarily determined by interaction with the conduction electrons. The magnitudes of T_1 agree fairly well with the Korringa theory in all three metals. The lithium data in particular indicate that $P_f/P_a \cong 0.6$. In lithium and sodium a dependence of T_1 on the resonance frequency is observed, which cannot be explained on the basis of the Korringa theory. Information about the atomic self-diffusion process is also obtained. Portions of the T_1 and T_2 data are interpreted using the theory of Bloembergen, Purcell, and Pound. In addition, some of the T_1 data are interpreted in terms of the lattice diffusion theory of Torrey. These analyses yield values for D, the coefficient of self-diffusion, of $0.24_{-0.10}^{+0.17} \times \exp(-13\,200 \pm 400/RT)$ cm²/sec in lithium and $0.20_{-0.15}^{+0.56} \times \exp(-10\,000 \pm 600/RT)$ cm²/sec in sodium. Although there is some ambiguity in the interpretation of the rubidium data, they indicate $D \cong 0.23 \exp(-9400/RT)$ cm²/sec. Unusual broadenings of the resonance lines are observed at the melting points in all three metals. These broadenings are not presently understood, but some features of the data can be correlated with a mechanism involving magnetic local fields which arise from lattice imperfections.

I. INTRODUCTION

THIS paper reports the results of a series of nuclear magnetic resonance experiments performed on three of the alkali metals, lithium, sodium, and rubidium, using the spin echo and induction decay techniques of Hahn.[1] The quantities which we have measured are the spin-lattice relaxation time T_1 and the spin phase-memory time T_2. ($T_2 \propto 1/\delta H$, where δH is the resonance line width.) These time constants have been observed over a range of temperatures from $-65°C$ to $250°C$, which includes the melting points of all three metals. Measurements were made at several values of the Larmor frequency in each metal.

Nuclear magnetic resonance (NMR) and electron spin resonance (ESR) measurements in metals have already yielded results of significance for the description of metallic properties. NMR measurements of the line shape, line width,[2-5] and paramagnetic shift of the resonance frequency[3-6] in metals and alloys have given information about the magnetic dipolar interactions of the metal nuclei among themselves and with the conduction electrons. In noncubic lattices, effects have been observed[5] which arise from interaction of the nuclear quadrupole moments with electric field gradi-ents existing at the lattice sites. From these measure-ments and others, information can be deduced about the coefficients of self-diffusion, the phase changes, and the electronic distributions in some metals and alloys. Recently, a combination of NMR and ESR measurements[7] in lithium has resulted in the first direct measurement of the electron spin contribution to the bulk susceptibility of a metal.

However, few measurements of T_1 have been reported. The only literature data seem to be some low-temperature measurements on aluminum,[8] copper,[9] and lithium[10] and room temperature data on copper.[11] Without T_1 data, the shift and line width measurements cannot be exploited so as to yield their full information content about the metallic lattice and the conduction electrons. The T_1 data have been lacking primarily because the usual values of T_1 in metals are inconveniently short for measurement by the "steady state" techniques.

In addition, line-width data have not been available for the narrow lines characteristic of cubic metals at temperatures near their melting points. These lines are typically narrower than the smallest easily achievable magnet inhomogeneities.

T_1 and T_2 in the alkalis fall generally between a few hundred microseconds and one second and are thus in a particularly convenient range for measurement with the pulse technique. The alkali metals were chosen for this work primarily because of their theoretical simplicity insofar as electronic properties are concerned. In addition, reported experiments[2,3] had already shown the existence of self-diffusion induced line width transitions in these metals. The low-melting points of the

1 E. L. Hahn, Phys. Rev. 80, 580 (1950).
2 H. S. Gutowsky, Phys. Rev. 83, 1073 (1951).
3 H. S. Gutowsky and B. R. McGarvey, J. Chem. Phys. 20, 1472 (1952).
4 H. S. Gutowsky and B. R. McGarvey, J. Chem. Phys. 21, 2114 (1953).
5 N. Bloembergen and T. J. Rowland, Acta Metallurgica 1, 731 (1953).
6 Townes, Herring, and Knight, Phys. Rev. 77, 852 (1950).
7 Schumacher, Carver, and Slichter, Phys. Rev. 95, 1089 (1954).
8 J. Hatton and B. V. Rollin, Proc. Roy. Soc. (London) A199, 222 (1949).
9 N. Bloembergen, Physica 15, 588 (1949).
10 N. J. Poulis, Physica 16, 373 (1950).
11 D. F. Abell and W. D. Knight, Phys. Rev. 93, 940(A) (1954).

alkalis made it possible to work with the molten metals using relatively crude thermal techniques. Measurements were not made in potassium because of its very small nuclear magnetic moment, which would result in prohibitively small nuclear signals with the present experimental arrangement. Measurements in cesium are planned for the future.

Some of the data on sodium which we report here have already appeared in preliminary form.[12]

II. APPARATUS AND MEASUREMENTS

A typical sample consisted of about 0.5 cc of an oil dispersion of metallic spheres sealed into a pyrex vial. The dispersions were produced by violent mechanical agitation of chunks of the metal in a high boiling point oil at a temperature slightly greater than the melting point of the metal. Average particle radii for the samples used were: lithium, 12μ, sodium, 25μ, and rubidium, 50μ. Typical samples contained an actual volume of about 0.1 cc of the metal. Several of the dispersions were prepared by Dr. T. R. Carver, and the rest supplied by Professor H. S. Gutowsky and his group in the chemistry department of the university.

Relaxation measurements were made using radio-frequencies between 3 and 15 Mc/sec. Over this range all but the rubidium samples have an average particle size smaller than the rf skin depth. It proved possible, using any of the samples, to achieve an rf pulse power setting such that there was no induction decay following the rf pulse. We may therefore infer that the rf attenuation arising from skin effects was quite small, since it was possible to produce rf magnetic fields of amplitude H_1 and pulse length t_w for which the magnetic moment nutational angle $\theta_1 = \gamma H_1 t_w$ was equal to π uniformly over substantially the entire sample volume. (γ is the nuclear gyromagnetic ratio. μ, the magnetic moment, is equal to $\gamma \hbar I$, where I is the nuclear spin.) Moreover, it can be shown that there will be no spurious effects on T_1 or T_2 of the type suggested by Bloembergen[13] even if the particles are large compared to the skin depth. These effects, for pulsed experiments, depend on the existence of appreciable diffusion of nuclei through the skin depth in times comparable to T_1 or T_2. The time to traverse one skin depth is about δ^2/D, where δ is the skin depth and D the diffusion constant. The largest values of D in the alkalis in the temperature

TABLE I. Spectrochemical analyses of the stock materials.

Sample	Percentages for all metallic impurities $\geq 0.01\%$
Lithium A	Na 0.3; Cu, Si 0.05
Lithium B	Na 4; Sb, Pb 0.05
Lithium (Li^6-enriched)	Ca, Fe, Ni 0.01
Sodium A	Li 0.1; Ca, Mg, Si, Sr 0.05
Sodium B	Li 0.4; Ca, Sr 0.1
Rubidium	(Not analyzed)

[12] R. E. Norberg and C. P. Slichter, Phys. Rev. **83**, 1074 (1951).
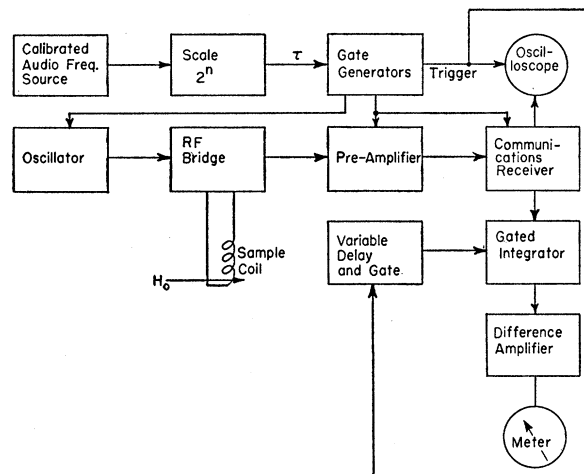[13] N. Bloembergen, J. Appl. Phys. **23**, 1383 (1952).

FIG. 1. Block diagram of the apparatus.

range involved here are perhaps 10^{-5} cm^2/sec (in the liquid phase). At temperatures corresponding to such a value of D, δ is in the vicinity of 50μ. Thus $\delta^2/D = 25 \times 10^{-6}/10^{-5} = 2.5$ sec. Since the largest values of T_1 or T_2 in this temperature region of large D are less than 0.1 sec, skin effects should be negligible.

The purity of the samples used was not especially good. Table I shows the results of spectrochemical analyses of the stock materials. Most of the lithium and sodium data were obtained with the A samples.

A copper-constantan thermocouple was laid against the outside wall of the sample vial and the rf coil then close wound directly onto the vial. For runs above room temperature, a constantan heater was wound noninductively on a card which was then wrapped around the sample. Temperatures below room temperature were attained by immersing the sample coil in a copper trough containing turpentine (whose dielectric constant is relatively insensitive to temperature over the temperature range involved). A coolant mixture of dry ice and acetone flowed through copper tubing soldered to the end walls and bottom of the trough. Temperatures between $-65°$ and $300°$C could be maintained and measured to $\pm 1°$C with these crude arrangements. The melting points of the lithium and sodium samples were checked calorimetrically by measuring time rate curves of heating and cooling, run with the samples situated in place in the magnet gap. The melting points observed were $97 \pm 1°$C for sodium (literature value $97.5°$C[14]) and $182 \pm 1°$C for lithium (literature value $180°$C[14]). The measured values varied by less than $2°$C between rapid-heating and rapid-cooling runs. During most of the T_1 and T_2 measurements, the thermal gradients over the samples were less than $1°$C.

The T_1 measurements were made by the application of two rf pulses. As the spacing between these pulses is

[14] C. J. Smithells, *Metals Reference Book* (Butterworth's Scientific Publications, London, 1949).
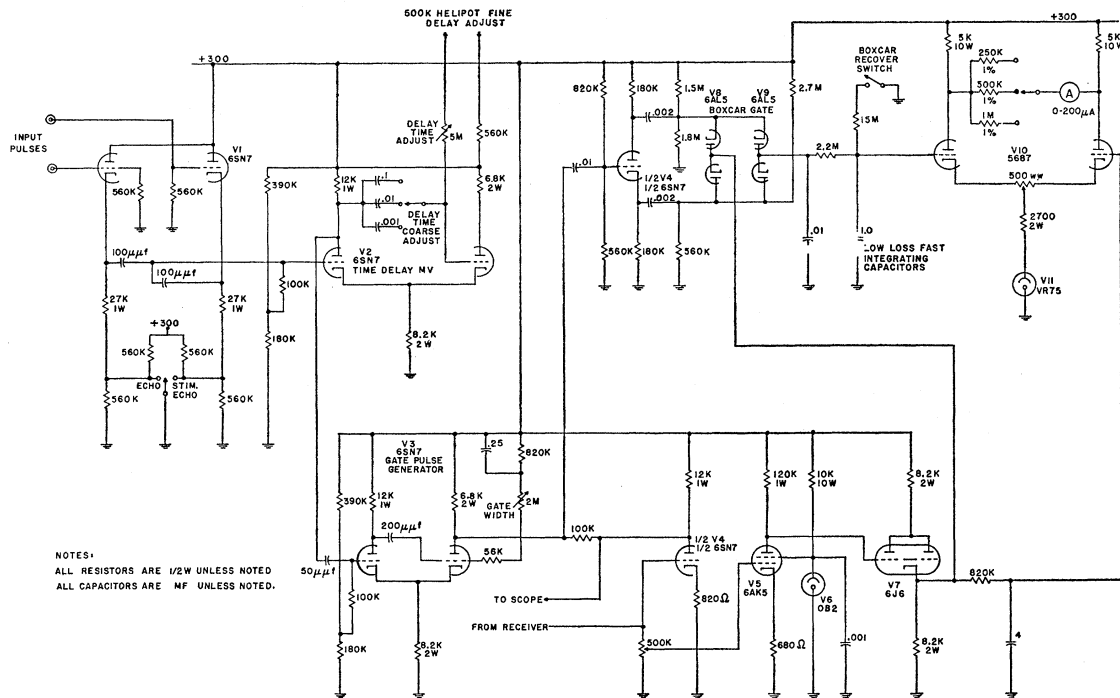
FIG. 2. Boxcar integrating circuit used to improve the signal-to-noise ratio. The necessary gating circuits are also shown in the left part of the figure.

increased, it is found that the initial amplitude of the free induction decay following the second pulse rises along an exponential curve with time constant T_1. The amplitude of the second decay reflects the degree of recovery of the nuclear spin system toward thermal equilibrium in the time interval between the first and second pulses. Most of the T_2 measurements were also made using two rf pulses, following the spin echo technique of Hahn.[1] The amplitude of the echo is observed as a function of the pulse spacing, the resulting exponential decay having time constant T_2. Some T_2 measurements were made using the technique of Carr and Purcell,[15] which is a modification of the Hahn method and involves the application of a series of pulses. The envelope of the echo decay may be observed by the application of a single Carr-Purcell pulse train.

The electromagnet and some of the radio-frequency apparatus have been outlined previously.[16] A block diagram of the experimental arrangement is shown in Fig. 1. A frequency-calibrated audio oscillator provides a basic timing wave which drives a scale of 2^n (where $n=1$ to 5). The interval output of the scaler is used as τ, the separation of the two rf pulses in the Hahn spin echo experiment. The scaler output initiates gate circuits which govern the rf pulses. The variable-frequency pulsed oscillator delivers rf pulses (typically 200 volts, 10 to 50 μsec duration) to a symmetrical twin-T rf bridge, one arm of which contains the sample

coil. The output from the bridge is amplified in a preamplifier having about a 100-kc bandpass and a voltage gain of 100. The preamplifier is a modification of the Wallman cascode design.[17] The amplified signal is detected in a communications receiver which has been broad-banded to be 3 db down at ± 15 kc. The preamplifier $B+$ voltage and the suppressor voltage on the first rf amplifier of the receiver are gated downwards during the rf pulse. This switching technique is necessary in order to avoid excessive overdriving of the rf amplifier stages.

The output of the second detector of the receiver is displayed on an oscilloscope and also fed into the electronic measuring circuit shown in Fig. 2. This measuring device is a "boxcar integrator"[18] and is, to a large extent, the work of L. S. Kypta and H. W. Knoebel. The essential operation is that of a cathode follower ($V7$) driving two channels; a reference channel containing a simple RC integrator, and a signal channel containing an electronic switch ($V8, 9$) in the form of a gated diode clamp. This gated diode clamp stage is followed by an RC integrator which utilizes very high leakage impedance condensers (polystyrene insulated). The integrated outputs of the two channels are placed on the input grids of a difference amplifier ($V10$) whose unbalance output is indicated on a meter. At each

15 H. Y. Carr and E. M. Purcell, Phys. Rev. 94, 630 (1954).
16 R. E. Norberg, Phys. Rev. 86, 745 (1952).

17 Wallman, Macnee, and Gadsden, Proc. Inst. Radio Engrs. 36, 700 (1948).
18 J. L. Lawson and G. E. Uhlenbeck, Threshold Signals, Massachusetts Institute of Technology Radiation Laboratory Series (McGraw-Hill Book Company, Inc., New York, 1950), Vol. 24.

repetition of the pulse array, the sampling channel places a charge on the 1.0-μf condenser. The charge is representative of the average signal occurring at $V7$ during the clamp gate. An equilibrium deflection of the output meter is achieved by sampling many pulse repetition intervals. As an example of the use of the circuit consider the method of measuring T_2 with the Hahn two-pulse technique. The two pulses are separated by an interval τ, and the echo occurs at time 2τ. The sampling gate interval is placed on the echo signal at time 2τ and the equilibrium meter deflection recorded. The gate interval is then placed at an arbitrary time on the noise baseline. The difference between the two readings is a measure of the echo amplitude. A plot of such amplitudes as a function of 2τ is exponential with logarithmic slope equal to T_2 if the spin system obeys the Bloch phenomenological equations.[1] Similarly, T_1 is measured by observation of the recovery of the free induction decay following the second rf pulse towards the equilibrium amplitude which corresponds to infinite pulse separation. The relative amplitudes of the decays are measured by automatically keeping the sampling gate at some time $\tau+\epsilon$ on the decay as the time of the second pulse, τ, is varied.

A comparison of the lithium and sodium data presented in Figs. 3 and 6 with those reported earlier[12] from photographic measurements made on similar samples shows the striking improvement of experimental accuracy provided by the gated integrator circuit. The device plays a narrow-banding third detector role for the measurement of transient nuclear resonance signals analogous to that which the familiar "lock-in"[19] plays for the signals of steady state experiments. Full exploitation of the instrument would demand the use of a stable, coherent rf oscillator followed by a gated power amplifier and the use of a phase-sensitive first detector. The difference amplifier could then deliver a center-null output. Our experiments involved amplitude detection of nuclear signals arising from the action of an incoherent pulsed oscillator. The absence of an rf carrier at the time of measurement of the nuclear signals meant that the detector characteristic was non-linear for small nuclear signals. It was necessary to prepare a calibration plot which provided detector corrections to be applied to each measurement.

The T_2 measurements using the technique of Carr and Purcell[15] were made as a check on the possible existence of diffusion-field inhomogeneity effects (Sec. III). For these measurements, R. L. Trogdon designed a pulser which provided the required arrays of pulses with $\theta_1=\pi/2$ and π. The Carr-Purcell T_2 runs were measured by either using the boxcar integrator or by photographing the oscilloscope display.

III. SUMMARY OF THE EXPERIMENTAL RESULTS

A brief outline of some of the experimental results obtained for Li[6], Li[7], Na[23], Rb[85], and Rb[87] is given at this point. Detailed analyses of the complete data for each isotope will be made in the subsequent sections. This initial summary is intended to emphasize the major similarities and differences among the data in the various metals.
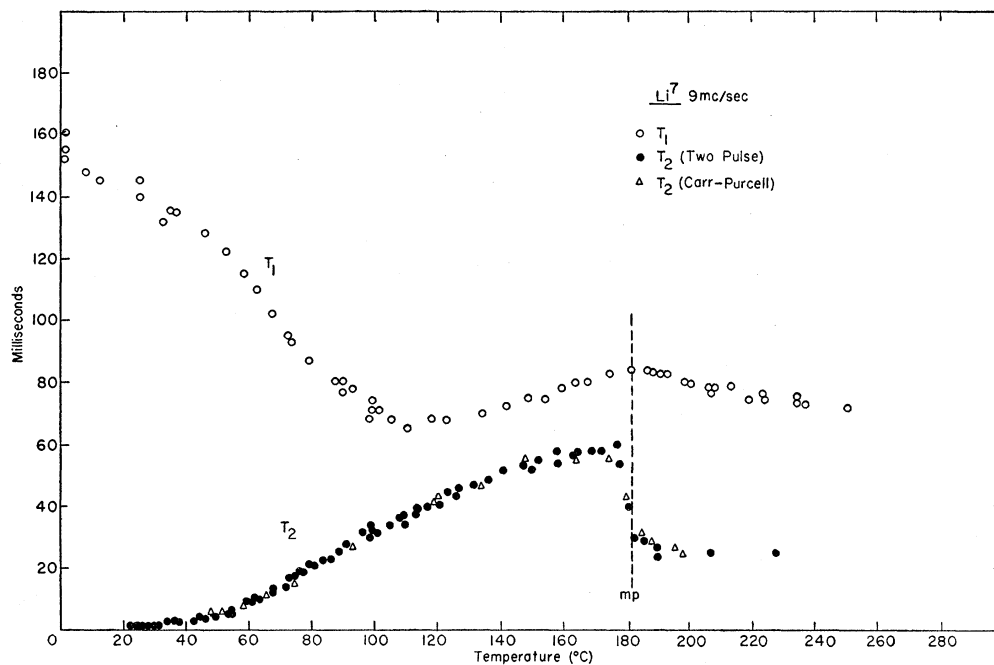

FIG. 3. T_1 and T_2 data for Li[7], measured in a sample of natural abundance, at a Larmor frequency of 9.0 Mc/sec.

[19] Bloembergen, Purcell, and Pound, Phys. Rev. 73, 679 (1948).

Figure 3 shows T_1 and T_2 obtained between 0°C and 250°C for the Li[7] resonance at 9.0 Mc/sec in a sample of natural isotopic abundance (92.1 percent Li[7], 7.9 percent Li[6]). T_1 is seen to decrease as the temperature is increased until about 110°C, where a minimum in T_1 occurs. Thereafter T_1 increases until 180°C, then decreases again for higher temperatures. This T_1 behavior will be shown in the next section to result from the superposition of two contributions to the nuclear relaxation. The first relaxation contribution arises from the interaction with the conduction electrons, is designated $(T_1)_e$, and should be inversely proportional to the absolute temperature. The second is a contribution from the direct nuclear dipole-dipole interaction, $(T_1)_d$. $(T_1)_d$ goes through a minimum at the temperature at which the inverse of the mean time which a diffusing nucleus spends at a given lattice site is of the order of ω_0, the Larmor angular frequency. The initial increase of T_2 with increasing temperature is a continuation of the line narrowing observed by Gutowsky and Mc-Garvey[3] to begin near 230°K. The narrowing line width in this region appears to arise entirely from the diffusion-limited nuclear dipolar interaction. T_2 increases until the T_1 contribution to T_2 becomes important [see Eq. (3), Sec. IV]. At the melting point a sharp reduction of T_2 occurs. This corresponds to a surprising broadening of the resonance line upon melting. The broadening is doubly unusual in that it is not accompanied by any associated T_1 decrease. The presence of the T_1 minimum at 110°C indicates that the correlation frequency for the self-diffusive motion has become much greater than the Larmor frequency by the time the melting point is reached, and therefore one would expect $T_1 \cong T_2$,[20] if the high-temperature interaction is able to produce nuclear relaxation. We return to this point in Sec. IV, C.

The complete T_1 and T_2 curves of Fig. 3 were reproducible for both samples A and B with no irreversible effects observed over the indicated temperature range. One possible source of a spurious broadening at a melting point is a suddenly increased rate of diffusion
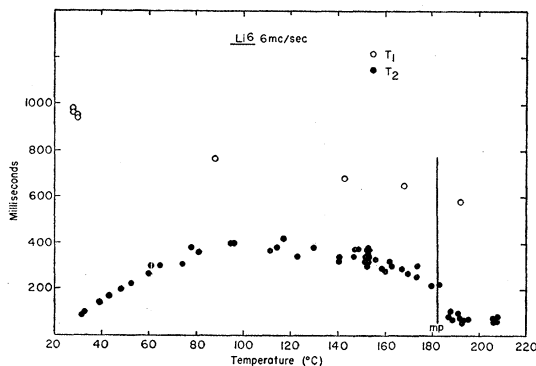
of the nuclei through the static inhomogeneous magnetic field distribution impressed over the sample by the magnet. The effect of such a process can be shown[1,16,21] to be an echo envelope decaying as $\exp(-t/T_2 - kt^3)$, where k is a constant involving the magnetic field gradient and the diffusion coefficient. The additional kt^3 term, if undetected, can result in misinterpretation of the data so as to yield T_2's substantially lower than the true values. Since there was evidence of non-exponential echo envelopes for lithium at high temperatures, check runs of the T_2 data were made by using the method of Carr and Purcell.[15] Their technique removes, in first order, the diffusion-inhomogeneity kt^3 term. The experimental results obtained with the Carr-Purcell technique are plotted as triangles in Fig. 3. The line-broadening at the melting point is shown to be real.

Figure 4 shows the results for Li[6] obtained at 6.0 Mc/sec in a sample enriched to 93.8 percent Li[6], 6.2 percent Li[7].[22] The accuracy of the data obtained from this sample does not approach that for Li[7] in natural abundance, but it is clear that T_1 decreases steadily as the temperature is increased, with no evidence of a minimum. As in Fig. 3, T_2 increases as the nuclear dipolar interaction averages out with increasing diffusion rate, and then levels off rather sooner, with respect to T_1, than in the Li[7] data above. At the melting

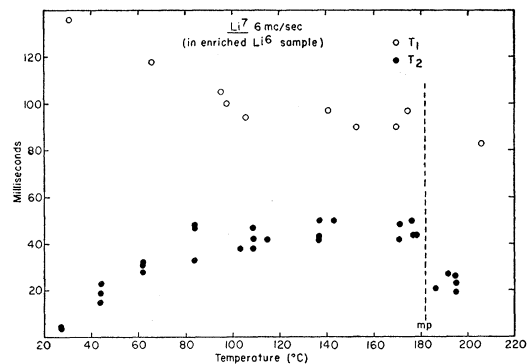FIG. 5. T_1 and T_2 data for Li[7] in the enriched Li[6] sample referred to in Fig. 4, at 6.0 Mc/sec.

point T_2 for Li[6] decreases suddenly, although somewhat less markedly than for Li[7].

Figure 5 shows data taken on the Li[7] resonance in this same Li[6]-enriched sample. The accuracy is very poor because of the small concentration of Li[7] nuclei in this sample, but it is seen that the general features of the data are similar to the data in Fig. 3, with two exceptions. The nuclear dipolar T_1 minimum is very much weaker because of the different nuclear environment. As in the case of the Li[6] data in Fig. 4, T_2 in the

FIG. 4. T_1 and T_2 data for Li[6], measured in a sample enriched to 94 percent Li[6], at 6.0 Mc/sec.

[20] R. K. Wangsness and F. Bloch, Phys. Rev. 89, 728 (1953).

[21] T. P. Das and A. K. Saha, Phys. Rev. 93, 749 (1954).
[22] We are indebted to the Stable Isotope Division of the Oak Ridge National Laboratory (U. S. Atomic Energy Commission) for supplying the enriched metal.

region just below the melting point is appreciably less than T_1.

Figure 6 shows 9.0-Mc/sec data for Na[23]. Here again, T_1 is in general inversely proportional to the absolute temperature, with a slight decrease occurring at the melting point. This reduction will be interpreted as reflecting the volume dependence of $(T_1)_e$. Most of the low temperature T_2 data in Fig. 6 have been published previously.[12] They extend to higher temperature the line-width transition reported by Gutowsky.[2] T_2 appears to become limited by T_1 near room temperature, and at the melting point displays a broadening similar to that observed in lithium. A few T_2 measurements were made in sodium using the Carr-Purcell technique and verified the T_2 behavior shown in Fig. 6.

Figure 7 shows data obtained for the Rb[85] and Rb[87] resonances in a sample of natural abundance (73 percent Rb[85] and 27 percent Rb[87]). Few T_2 points were measured because of experimental limitations at the short T_2 values in rubidium and because of rather poor

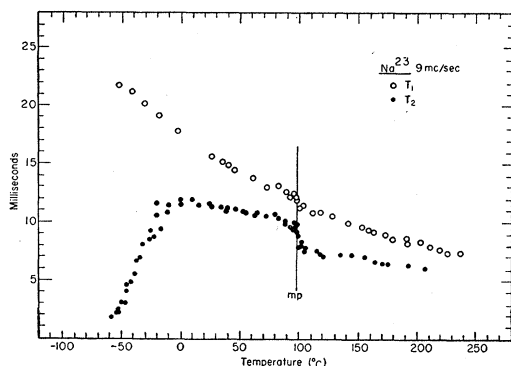FIG. 6. T_1 and T_2 data for Na[23] at 9.0 Mc/sec.

signal-to-noise ratios. The data in the two isotopes were taken at about the same magnetic field (7500 oe), corresponding to Larmor frequencies of 3.0 Mc/sec for Rb[85] and 10.5 Mc/sec for Rb[87]. The Rb[87] data show a T_1 minimum near 0°C. The dashed curve indicates T_2 corresponding to the Rb[87] line width data of Gutowsky and McGarvey[4] and the assumption of a Lorentz line shape, that is, the absorption as a function of frequency is assumed proportional to $1/[1+T_2{}^2(\omega-\omega_0)^2]$, where ω_0 is the Larmor angular frequency. Above the melting point T_1 is inversely proportional to the absolute temperature within the large experimental scatter. In the liquid, T_2 is equal to T_1 within the error of the observations.

In Rb[85] the low-temperature T_1 data are qualitatively similar to those in Rb[87], with the minimum shifted (as it should be for lower Larmor frequency) towards lower temperature, and lying beyond the range of measurements. T_2 presumably equals T_1 below the melting point, but there are no reliable T_2 data. Again, T_1 decreases with increasing temperature above the melting point, and appears to be entirely $(T_1)_e$. In Rb[85],

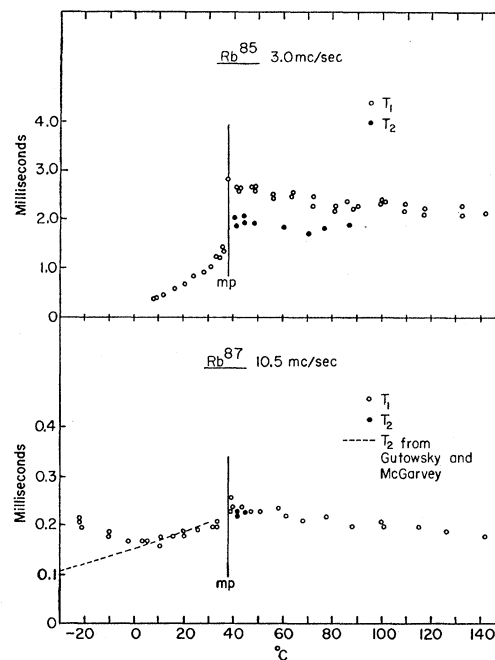FIG. 7. T_1 and T_2 for a rubidium sample of natural isotopic abundance, 73 percent Rb[85] and 27 percent Rb[87]. The Rb[85] measurements made at 3.0 Mc/sec and the Rb[87] measurements made at 10.5 Mc/sec correspond to roughly the same value of H_0, the applied static magnetic field.

T_2 in the liquid metal is significantly less than T_1, which indicates the presence of a line broadening similar to that observed in molten lithium and sodium.

Some significant common features of the data in all of the alkalis investigated are a behavior of T_2 near room temperature which reflects a diffusion-induced transition of the dipolar line width, T_1 generally proportional to $1/T$ with several instances of the occurrence of T_1 minima, and an unexpected high-temperature line-width term, very pronounced in lithium, less so in sodium, and visible in rubidium only as an extra broadening in one isotope.

IV. INTERPRETATION OF THE EXPERIMENTAL RESULTS

In the subsequent sections we shall attempt to separate and examine the interactions arising from several sources. In general, we shall assume that an observed spin-lattice relaxation time is the resultant of contributions from a number of lifetime-limiting processes whose effects add as transition probabilities, i.e.

$$1/T_1 = \sum_i (1/T_1)_i. \tag{1}$$

If all the interactions which contribute significant line broadenings correspond to the same line shape, then the line widths add and

$$1/T_2 = \sum_i (1/T_2)_i. \tag{2}$$

Each line-width term may be further reduced to the

sum of a static broadening $(1/T_2')$, which arises from the essentially constant local fields, and a quantum indeterminacy broadening associated with the spin state lifetime T_1,[19] that is,

$$(1/T_2)_i = (1/T_2')_i + (1/2T_1)_i. \qquad (3)$$

The combination of (2) and (3) permits the separation of the individual static line width terms,

$$\left(\frac{1}{T_2'}\right)_i = \frac{1}{T_2} - \left(\frac{1}{2T_1}\right)_i - \sum_{j \neq i}\left(\frac{1}{T_2}\right)_j. \qquad (4)$$

A. Interaction with the Conduction Electrons

We begin the detailed examination of the data by considering the interaction of the nuclei with the conduction electrons. Heitler and Teller[23] pointed out in 1936 that there should be a very potent relaxation process for the nuclear magnetic moments in a metal via a spin-spin interaction with the conduction electrons.

The Hamiltonian describing the magnetic interaction of the nucleus with the conduction electrons is discussed by Bloembergen and Rowland.[5] There are three main terms in the interaction, the $I \cdot S$ hyperfine nuclear spin-electron spin term which occurs because of the finite value of the electron wave function at the position of the nucleus, the "outside" nuclear spin-electron spin interaction, and a nuclear spin-electron orbit term. The first term is generally by far the largest, and gives rise to a strong relaxation process for the nuclei. Another observable effect of the hyperfine interaction upon the nuclear magnetic resonance in a metal is a paramagnetic shift of the resonance frequency for a nucleus in the metal with respect to the resonance frequency for the same nuclear species in an isolated atom (usually approximated experimentally by a salt).[24] Townes, Herring, and Knight[6] have shown the shift to be a measure of the electron spin contribution to the magnetic susceptibility of the metal, that is,

$$\frac{\Delta H}{H_0} = \frac{8\pi}{3}\chi_a P_f = \frac{I}{2I+1}\frac{\Delta E}{\mu_e\mu_n}\chi_a\frac{P_f}{P_a} \qquad (5)$$

in which ΔH is the shift of the resonance frequency and H_0 is the applied static magnetic field. χ_a is the electron spin contribution to the susceptibility per atom, ΔE is the hyperfine splitting of the ground state of the free atom, P_f is the probability density evaluated at the nucleus for an electron in the Fermi surface, and P_a is the probability density at the nucleus for the valence electron in the free atom.

In 1950, Korringa[25] and, independently, Slichter[26] examined the relation between the shift $\Delta H/H_0$ and

[23] W. Heitler and E. Teller, Proc. Roy. Soc. (London) A155, 629 (1936).
[24] W. D. Knight, Phys. Rev. 76, 1259 (1949).
[25] J. Korringa, Physica 16, 601 (1950).
[26] C. P. Slichter (unpublished).

$(T_1)_e$, the electron contribution to the nuclear spin-lattice relaxation time. Korringa performed a first-order perturbation calculation, using Bloch wave functions for the electrons. The diagonal matrix elements of the Hamiltonian are responsible for the paramagnetic or "Knight" shift, and the off-diagonal terms give the transition probabilities between adjacent m-levels of the nucleus and thus determine $(T_1)_e$.

The nuclear spin-electron orbit term in the Hamiltonian vanishes to first order because of the local electric fields which quench the orbital angular momentum of the electrons in the metal. The quenching should be complete except for a small effect arising from the electron spin-orbit interaction. The spin-spin terms outside the nucleus should be small compared to the hyperfine term, especially so in the alkalis where P_f is rather large. Korringa's result for $(T_1)_e$, considering only the hyperfine interaction, may be written

$$\frac{1}{(T_1)_e} = \frac{4\pi kT}{\hbar}v_0^2\rho^+(\epsilon_0)\rho^-(\epsilon_0)\left(\frac{P_f}{P_a}\frac{\Delta E}{2I+1}\right)^2, \qquad (6)$$

where $\rho^\pm(\epsilon_0)$ are the densities of electron states per unit volume per unit energy for spins up and down respectively, evaluated at the Fermi surface, and v_0 is the atomic volume. Korringa also considered the outside spin-spin and the nuclear spin-electron orbit contributions, which give rise to small terms in addition to (6). $(T_1)_e$ is predicted by (6) to be inversely proportional to the temperature and to be substantially independent of the applied static magnetic field H_0. These features are not changed by the addition of the aforementioned extra terms to (6). In a magnetic field the Fermi surfaces for electrons of spin up and spin down are separated by an energy $2\gamma_e\hbar H_0$, so there is a small dependence of $\rho^+(\epsilon_0)$ and $\rho^-(\epsilon_0)$ on H_0. However, $\gamma_e\hbar H_0$ is only about 0.01 percent of the Fermi energy ϵ_0, and the effect on $(T_1)_e$ should be very small indeed.

Korringa's result for the Knight shift, also calculated in the free electron approximation, is

$$\frac{\Delta H}{H_0} = \frac{\gamma_e\Delta E}{\gamma_n(2I+1)}v_0\rho^+(\epsilon_0)\frac{P_f}{P_a}. \qquad (7)$$

Combination of (6) and (7) leads to what is usually referred to as the "Korringa relation,"[25,26]

$$T_1\left(\frac{\Delta H}{H_0}\right)^2 = \frac{\hbar\gamma_e^2}{\pi kT4\gamma_n^2}. \qquad (8)$$

It should be noted that Overhauser[27] has derived an expression for $(T_1)_e$ by a slightly different method, and his result agrees exactly with (6).

In addition to the magnetic interactions, there could be a significant coupling between the quadrupole mo-

[27] A. W. Overhauser, Phys. Rev. 89, 689 (1953).

ment of a nucleus with spin ≥ 1 and an electric field gradient at the nucleus arising from the conduction electrons. Such a term has been discussed by Bloembergen and Rowland,[5] but should be negligible for the cubic alkali metals.

Figures 8 through 11 show T_1 data in the various metals, plotted as a function of the reciprocal of the absolute temperature. The plotted points differ slightly from the experimental data given in Sec. III in that T_1 has been corrected for the volume dependence of $(T_1)_e$ as given by (6). The product $v_0^2 \rho^2$ is proportional to $v_0^{4/3}$ in the free electron approximation. Because of thermal expansion of the metal, this introduces a small temperature dependence into (6) in addition to the general $1/T$ behavior of $(T_1)_e$. This small additional temperature dependence has been removed, normalizing to the experimental points at 25°C in lithium and sodium and at 40°C in rubidium. Coefficients of thermal expansion were taken from the literature.[28] Equation (8) predicts that the product $T_1(\Delta H/H_0)^2$ should be proportional to $1/T$ with no volume dependence. If the sodium T_1 data of Fig. 6 are so combined with the literature shift values,[4] the results agree with the 9-Mc/sec data of Fig. 10.

The straight lines in the figures are drawn with the inverse temperature dependence predicted by (6), normalized to the experimental points at room temper-
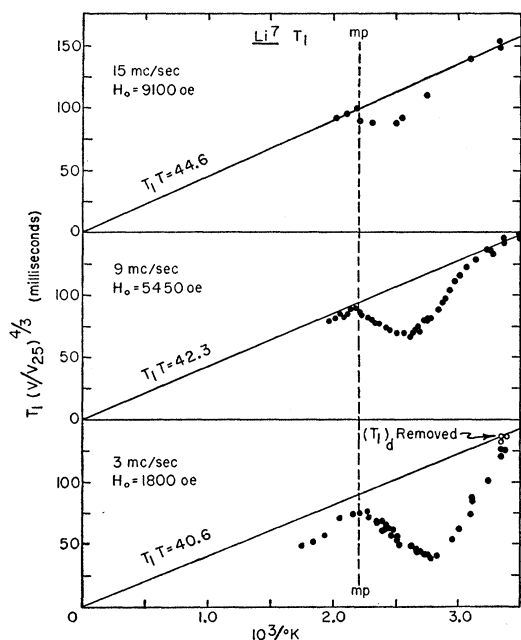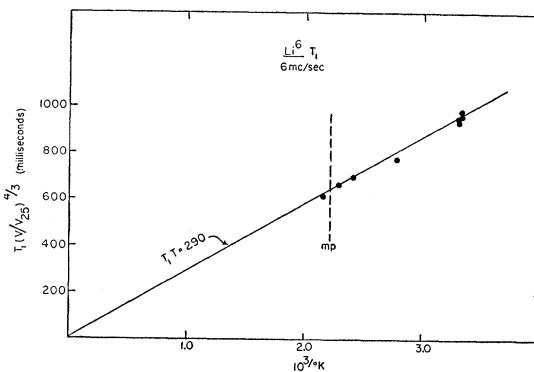

FIG. 9. T_1 data for Li[6], adjusted to remove the $v_0^{-4/3}$ dependence and plotted against reciprocal temperature. The straight line is determined as in Fig. 8.

ature in lithium and sodium, and at 40°C in rubidium. It is evident that the major T_1 contributions in these metals are indeed inversely proportional to the absolute temperature. One also notices that in Li[7] and Na[23] there is a 5 to 10 percent variation of the entire T_1 curve as the magnetic field H_0 is changed by a factor of 3. This point will be considered later in this section.

Table II presents a correlation of the experimental T_1 data with the theoretical expressions (6) and (8). Values for lithium and sodium are taken at 300°K, where the temperature dependence and other considerations indicate that the contribution to the experimental T_1 from interactions other than that with the electrons is small. For the same reason, values for rubidium are taken at 40°C, just above the melting point.

$(T_1)_e$ is calculated from Eq. (6) by using the available theoretical values of m/m^* and P_f/P_a, as indicated in the table. The free electron approximation is modified only to the extent of the use of an effective mass in the evaluation of $v_0\rho$. [$v_0\rho = 3/(4\epsilon_0)$ and $\epsilon_0 = \hbar(3\pi^2/v_0)^{\frac{2}{3}}/2m^*$.] The general result is that (6) is fairly successful in predicting T_1 when an m^* is used. It should be noted that we have ignored possible effects of correlations among the electrons upon the density of states ρ. A recent calculation by Pines[29] indicates that ρ might be affected to perhaps 10 percent by electron correlation and exchange.

The results for Li[6] and Li[7] are mutually consistent when values at constant v_0 are compared. [The $(\Delta E/(2I+1))^2$ term in (6) means that $(T_1)_e$ should be proportional to γ_n^{-2}.] The Rb[85] and Rb[87] results are also in good mutual agreement.

The value for P_f/P_a in lithium is from a recent recalculation by Kohn with an improved method. The previous value was 1.0.[30] The T_1 data at 15.0 Mc/sec, if taken to represent $(T_1)_e$, indicate that $P_f/P_a \cong 0.6$. The measured T_1's are all somewhat smaller than the values predicted by (6). The consistent discrepancy

FIG. 8. T_1 data for Li[7], taken at three values of the Larmor frequency and adjusted to remove the $v_0^{-4/3}$ dependence predicted by Eq. (6). The data are plotted against the reciprocal of the absolute temperature in units of $10^3/°K$. The straight lines are drawn with the $1/T$ dependence predicted by Eq. (6) and normalized to the data at 300°K.

[28] *International Critical Tables* (McGraw-Hill Book Company, Inc., New York, 1933).

[29] D. Pines (private communication).
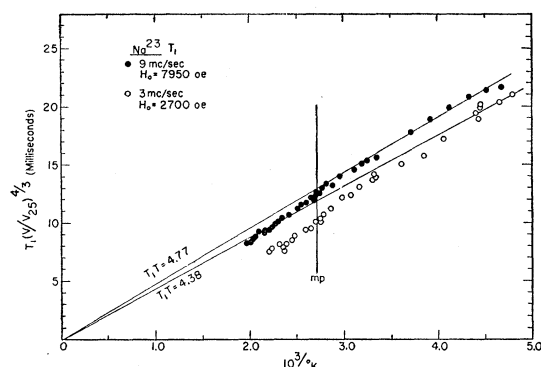[30] W. Kohn and N. Bloembergen, Phys. Rev. **80**, 913 (1950); Phys. Rev. **82**, 283 (1951).

FIG. 10. T_1 data for Na[23], taken at two values of the Larmor frequency, adjusted to remove the $v_0^{-4/3}$ dependence and plotted against reciprocal temperature. The straight lines are determined as in Fig. 8.

may indicate the presence of an additional relaxation term, and is discussed at the end of this section.

Inspection of the final columns of Table II reveals that the "Korringa relation" (8) yields consistently low T_1's. It should be noted that this discrepancy is in the opposite direction to the effect to be expected if the terms omitted from (6) actually contributed to $(T_1)_e$. If these terms were important, the experimental T_1's would be shorter than those predicted by the Korringa relation. Equation (7), which is more successful, particularly in sodium, is one of the two expressions involved in (8). A check calculation of the shifts predicted by (7) shows that the discrepancy found between experiment and the results of (8) is also present in (7). The measured alkali shifts are all larger than (7) would predict. The Townes, Herring, and Knight expression (5) for the shift is in very good agreement with the measured shifts if current measured[7,31] or theoretical χ_a values are used. In lithium, in particular, the recently measured[7] χ_a agrees with Pines'[32] calculated value and both coincide with χ_a calculated from $\Delta H/H_0$. The failure of (7) seems to arise from the fact that a free electron calculation of the spin susceptibility, even using an effective mass, is not adequate. It should be noted that (7) becomes more successful with increasing Z.

The Li[7] data, Fig. 8, are particularly interesting in that the T_1T product of about 45 is very different from the results of Poulis[10] at low temperatures. He has observed a dependence on v_0 qualitatively similar to ours, although even more pronounced. However, comparing our 15.0-Mc/sec data with Poulis's results at 15.4 Mc/sec (at which frequencies both sets of data are most nearly proportional to $1/T$) one finds his T_1T at 20°K to be about 25 sec deg as compared with our 45. Although Poulis used the "saturation method"[19] described by Bloembergen, in which there exists the

[31] S. R. Rao and K. Sarithri, Proc. Indian Acad. Sci. 6, 207 (1942).
[32] D. Pines, Phys. Rev. 95, 1090 (1954).

possibility of a calibration error, such an error seems unlikely since Poulis was able to make direct observations of recovery to equilibrium for the longer T_1's as a check on his calibration. The other possibility is a peculiar plateau of the T_1 against T plot between 20°K and 273°K, which seems even more unlikely. Unfortunately, experimental limitations on measurements at short T_2's prevented us from measuring T_1 at liquid nitrogen temperature.

It is difficult to reconcile a significant dependence of $(T_1)_e$ upon the applied static field or the resonance frequency with Eq. (6). As previously pointed out, the only field dependence of $(T_1)_e$ arising from the $\mathbf{I} \cdot \mathbf{S}$ hyperfine term lies in the small effect of H_0 upon the product $\rho^+(\epsilon_0)\rho^-(\epsilon_0)$, and this effect should be completely negligible. Even if the dipole-dipole or spin-orbit contributions to $(T_1)_e$ were appreciable, they should be independent of H_0. It is even more difficult to account for the observed effect in terms of a dependence of $(T_1)_e$ upon v_0, since the correlation frequency describing the motion of the conduction electrons is much greater than v_0, and changes in v_0 should not affect the efficacy of the interaction.

There is one piece of information from the data of Table II which indicates that we are dealing with a dependence of T_1 upon the resonance frequency rather than the applied field, H_0. Consider the relative magnitudes of T_1 measured for Li[6] and Li[7]. The results at 300°K are: for Li[6] at 6.0 Mc/sec and 9600 oe, $T_1 = 965$ msec; for Li[7] at 6.0 Mc/sec and 3600 oe, $T_1 = 138$ msec; and for Li[7] at 15.0 Mc/sec and 9100 oe, $T_1 = 150$ msec.
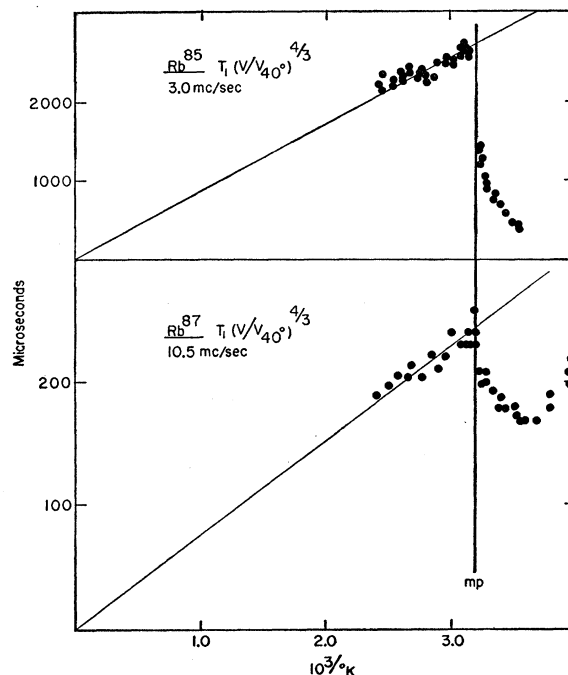

FIG. 11. T_1 data for the rubidium isotopes, with the $v_0^{-4/3}$ dependence removed from the data above the melting point, plotted against reciprocal temperature.

TABLE II. Comparison of experimental and theoretical values of $(T_1)_e$.

	Experiment				Theory Korringa T_1 expression Eq. (6)			"Korringa relation" Eq. (8)	
	ν_0 Mc/sec	H_0 oersteds	T °K	T_1 msec	m/m^{*a}	P_f/P_a	$(T_1)_e$ msec	$\Delta H/H_0^b$	$(T_1)_e$ msec
Li⁶	6.0	9600	300	965±35	0.69	0.5c	1590		(616)
Li⁷	15.0	9100	300	150±5	0.69	0.5c	227	2.61×10⁻⁴	88
	9.0	5400		141					
	6.0	3600		138					
	3.0	1800		(136)					
Na²³	9.0	8000	300	15.9±0.3	1.02	0.81d	16.8	11.2×10⁻⁴	10.3
	3.0	2700		13.9					
Rb⁸⁵	3.0	7300	313	2.75±0.2	1.12	1.0e	3.3	65×10⁻⁴	2.1
Rb⁸⁷	10.5	7500	313	0.245±0.02	1.12	1.0e	0.29	65×10⁻⁴	0.18

a H. Brooks (private communication to D. Pines), reference 32.
b See reference 3.
c W. Kohn, Phys. Rev. 96, 590 (1954). We are indebted to Dr. Kohn for communicating his results to us prior to publication.
d See reference 6.
e Estimated.

In none of these values does there appear to be a significant $(T_1)_d$ contribution (see Sec. IV, B). From (6), $(T_1)_e$ should be proportional to γ_n^{-2}. $\gamma_7^2/\gamma_6^2 = 7.0$, therefore the measured Li⁶ value predicts a $(T_1)_e$ of 138 msec for Li⁷. The γ_n^{-2} dependence seems to hold for constant ν_0 rather than constant H_0. The experimental value for Li⁷ at 9100 oe, even assuming the maximum error, corresponds to a minimum value for $(T_1)_e$ of 1020 msec, which is outside the error on the Li⁶ T_1 at 9600 oe.

One additional feature of the apparent frequency dependence should be noted. The volume-corrected T_1 curves pass smoothly through the melting point in sodium, and appear to do so in lithium. If the frequency or field dependence arises from any interaction involving the lattice, one would expect a break in the T_1 curve at the melting point. The conduction electrons appear to be the only likely source of an interaction which is insensitive to melting, but the frequency or field dependence probably arises from some interaction other than those which have been mentioned.

B. Effects of Self-Diffusion: Dipolar T_1 and T_2

We now turn to the effects of lattice diffusion on T_1 and T_2 in the alkali metals. A general theory of the T_1's and T_2's which result from interactions of the nuclei with fluctuating local magnetic fields has been given by Bloembergen, Purcell, and Pound[19] and in Bloembergen's thesis.[33] (The Bloembergen, Purcell, and Pound paper will be referred to as BPP in the following.) We will be interested in the BPP theory as it relates to nuclear dipole-dipole interactions and the effects of diffusional motion of the nuclei. The BPP theory was developed in detail for the case of isotropic liquid media, but many of the results are valid for the body-centered cubic lattice of the alkalis. We will also make use of a more complete theory developed by Torrey[34] for T_1 in the case of translational diffusion in a lattice.

[33] N. Bloembergen, Nuclear Magnetic Relaxation (Martinus Nijhoff, The Hague, 1948).
[34] H. C. Torrey, Phys. Rev. 92, 962 (1953).

BPP consider the case in which the local magnetic fields at one nuclear site arise from surrounding nuclear dipoles of the same species. The BPP expression for the contribution to the line width from essentially static local fields is

$$\left(\frac{1}{T_2'}\right)_d = \frac{3}{2}\gamma^2\hbar\left(\frac{I(I+1)}{3}\frac{1}{2\pi}\int_{-2/T_2'}^{2/T_2'}J_0(\omega)d\omega\right)^{\frac{1}{2}}, \quad (9)$$

where J_0 is the Fourier transform of the time spectrum of dipolar local fields. The subscript d indicates nuclear dipolar fields as the source of the interaction. For the case of interaction with only one nearest neighbor, Bloembergen[33] obtains

$$\left(\frac{1}{T_2'}\right)_d = \left[\frac{6}{5}\gamma^4\hbar^2\frac{I(I+1)}{b^6}\frac{1}{2\pi}\int_{-2/T_2'}^{2/T_2'}\frac{\tau_c}{1+\omega^2\tau_c^2}d\omega\right]^{\frac{1}{2}}, \quad (10)$$

where τ_c is a correlation time for the relative motion of the nuclei and b is the internuclear distance. The theory has been extended slightly to the case of a homogeneous distribution of nuclear dipoles,[35] and, in this case, one has

$$\left(\frac{1}{T_2'}\right)_d = \frac{3}{2}\gamma^2\hbar\left(\frac{I(I+1)}{3}\frac{1}{2\pi}\right.$$

$$\left.\times\int_{-2/T_2'}^{2/T_2'}\int_{r=a}^{\infty}\frac{32\pi N}{5r^4}\frac{\tau_c}{1+\omega^2\tau_c^2}drd\omega\right)^{\frac{1}{2}}, \quad (11)$$

where the r-integration is taken from a minimum nuclear impact parameter a. For translational diffusion, the correlation time may be written $\tau_c = r^2/12D$, where D is the diffusion coefficient, $D_0\exp(-E_D/RT)$. N is the number of nuclei per unit volume. Only the low-frequency components of J_0 enter into expression (9) for T_2'. The effective components are those for which $\omega^2\tau_c^2 \leqslant (2/T_2')^2\tau_c^2 \ll 1$. Using this fact, one obtains

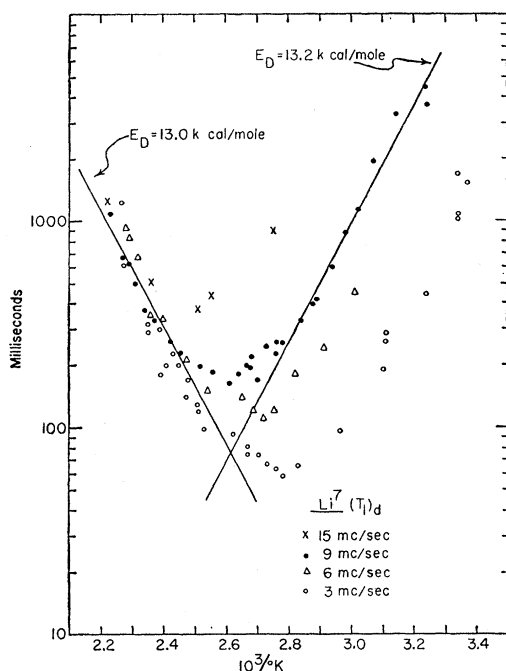[35] R. E. Norberg, thesis, University of Illinois, 1951 (unpublished).

FIG. 12. $(T_1)_d$ for Li^7 at four different frequencies, plotted against reciprocal temperatures, showing the minimum in $(T_1)_d$ and the shift of the minimum with frequency. The straight lines are least-squares fits of those 9-Mc/sec data which lie outside the region of the curved minimum.

$J_0(\omega) = 8\pi N/12Da$ and, from (9),

$$(1/T_2')_d = 4\gamma^4\hbar^2 I(I+1)N/5Da. \tag{12}$$

In the case of the b.c.c. alkali lattices, a will be taken as the nearest neighbor distance.

The fluctuating local fields also produce spin-flipping if the characteristic frequency of the fluctuations is in the vicinity of the Larmor frequency. The flipping provides a spin-lattice relaxation process since magnetic energy is exchanged with the energy of lattice motions. By a method similar to that used in deriving Eq. (11), BPP obtain

$$\left(\frac{1}{T_1}\right)_d = \frac{5\pi}{3}N\gamma^4\hbar^2 I(I+1)\int_a^\infty \frac{1}{r^4}\left\{\frac{\tau_c}{1+\omega_0^2\tau_c^2}\right.$$
$$\left.+\frac{2\tau_c}{1+4\omega_0^2\tau_c^2}\right\}dr. \tag{13}$$

From (13) the important features of the T_1 behavior may be seen. At low temperatures we have the relation $\omega_0^2\tau_c^2\gg1$, therefore $T_1 \propto \tau_c$. Again using $\tau_c = r^2/12D$ and integrating (13), we obtain

$$(1/T_1)_d = 144\pi\gamma^4\hbar^2 I(I+1)ND/25\omega_0^2 a^5 \tag{14}$$

for this region of low temperatures. $(T_1)_d$ is inversely proportional to D, and therefore decreases exponentially as the temperature increases. When a temperature is reached such that $\omega_0\tau_c = 1/\sqrt{2}$, Eq. (13) gives a

minimum value for $(T_1)_d$. At higher temperatures where $\omega_0^2\tau_c^2 \ll 1$, if we again substitute for τ_c and integrate (13), the result is

$$(1/T_1)_d = 2\pi\gamma^4\hbar^2 I(I+1)N/5Da, \tag{15}$$

so that $(T_1)_d$ is now proportional to D and increases exponentially as the temperature goes toward ∞.

1. Lithium

Let us first examine the Li^7 T_1 minimum. To represent the combination of $(T_1)_e$ and any frequency-dependent $(T_1)_x$ which may exist, we select a smooth curve drawn through the T_1 data at room temperature and those just above the melting point. The curve is nearly proportional to $1/T$ and includes a small decrease at the melting point corresponding to the volume change. The $(T_1)_d$ data resulting from the reciprocal subtraction corresponding to Eq. (1) are shown in Fig. 12. The asymptotic form of the extremes of the minima is seen to be exponential, in agreement with (14) and (15). A least-squares fit of the 9.0-Mc/sec data yields the activation energies indicated. The displacement of the temperatures T_m at which the minima occur as a function of the Larmor frequency ω_0, is well fitted by the relation $\ln\omega_0 \propto -E_D/RT_m$, which arises from the condition that $\omega_0\tau_c$ be equal to a constant at the minimum and the assumption that $\tau_c \propto \exp(-E_D/RT)$. A semilog plot of the frequencies against $1/T_m$ is exponential with a slope of about 13 kcal/mole. The minimum $(T_1)_d$'s are proportional to ω_0, which is a general result for motional relaxation, independent of a detailed theory.

In order to determine a diffusion coefficient from the $(T_1)_d$ data, we consider first the high-temperature region, where the relation $\omega_0^2\tau_c^2 \ll 1$ holds. Here, Eq. (15) is independent of the shape of the cutoff of the spectrum of local fields and is thus unaffected by the particular choice of correlation function. If we take $a = 3.02$ A (the nearest-neighbor distance in lithium), $N = 4.37 \times 10^{22}$/cc [from N(b.c.c.) $= 2/$(lattice parameter)$^3 \times$ percent abundance of Li^7], and the measured $(T_1)_d$ of 0.58 sec at $10^3/°$K $= 2.30$, we obtain $D = 5.0 \times 10^{-8}$ cm^2/sec. If we accept 13.2 kcal/mole as the activation energy (see T_2' data below), this result corresponds to $D = 0.23 \exp(-13\,200/RT)$. The contribution of the 8 percent of Li^6 moments to $(T_1)_d$ and $(T_2')_d$ can be shown to be about 0.3 percent, and it has been neglected in the above considerations. On the low-temperature side of the minimum, (14) fails to yield results consistent with the data. Using $D = 0.23 \exp(-13\,200/RT)$, Eq. (14) predicts $(T_1)_d = 4.3$ sec at $10^3/°$K $= 3.00$ and 9.0 Mc/sec, whereas the observed value is 0.95 sec. It is to be noted that (14) depends upon the choice of correlation function and, because of the a^5 dependence, is very sensitive to a choice of minimum impact parameter.

Torrey^{34} has extended the BPP theory to a more precise computation of $(T_1)_d$ for specific cases of trans-

lational lattice diffusion. Assuming that the self-diffusion process consists of a random walk with uniform flight path distance l, his result [reference 34, Eq. (86)] is

$$\left(\frac{1}{T_1}\right)_d = \frac{8\pi}{5}\gamma^4\hbar^2 I(I+1)\frac{n}{k^3 l^3 \omega}\Psi(k,y), \qquad (16)$$

where we take l to be the nearest neighbor distance, and $\Psi(k,y)$ is a function which Torrey has tabulated for a f.c.c. lattice. Using the proper Ψ tabulation for a b.c.c. lattice[36] (for which $k=0.763$), we have applied the theory to the Li^7 data. The method of analysis was to normalize the data of Fig. 12 by forming the ratio $T_1/(T_1)_{\text{minimum}}$ and determine the corresponding $\omega_0\tau/2$ from the tabulated functions. A plot of $\omega_0\tau/2$ against $1/T$ is shown in Fig. 13, corresponding to the 3.0-Mc/sec data of Fig. 12. The analyzed data closely follow an exponential curve, with the indicated activation energy of 13.2 kcal/mole. It should be noted that Torrey uses $\tau=r^2/6D$, so that his τ is equal to twice the τ_c used here.

Torrey's expression, (16), in its low-temperature asymptotic form, provides a better agreement with the observed $(T_1)_d$ than does Eq. (14) from the BPP theory. At $10^3/°K=3.00$, where the 9.0-Mc/sec $(T_1)_d$ is measured to be 0.95 sec, the Torrey expression, with $D=0.24\exp(-13\,200/RT)$, predicts $(T_1)_d=1.2$ sec. As
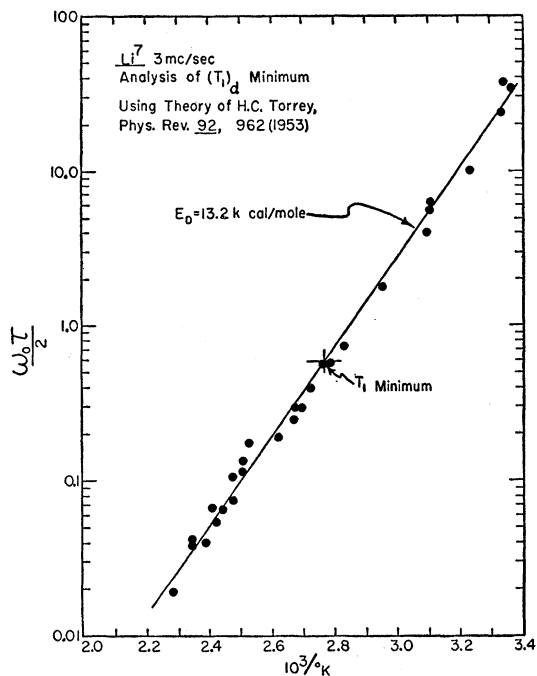

FIG. 13. Plot of $\omega_0\tau/2$ against reciprocal temperature, obtained from analysis of $(T_1)_d$ data for Li^7 at 3 Mc/sec from Fig. 12 using the Torrey theory.

[36] H. C. Torrey, Phys. Rev. 96, 690 (1954). We are indebted to Professor Torrey for providing us with the b.c.c. tabulations of his functions in advance of publication.
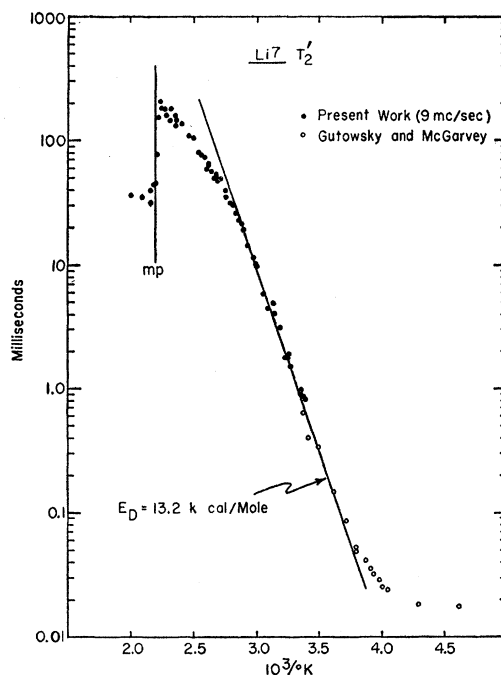

FIG. 14. T_2' for Li^7, calculated from the data of Fig. 3 using Eq. (17) and plotted against reciprocal temperature. The straight line is a best fit of the data in the region of the exponential dependence of T_2' on temperature.

stated previously, Eq. (14) gives 4.3 sec. The BPP and Torrey theories both successfully fit the moderately high temperature $(T_1)_d$ data, for which $\omega_0^2\tau_c^2\ll1$. Here the effective local fields near ω_0 arise primarily from remote nuclei, since the neighboring nuclei contribute mainly very high frequency terms. On the other hand, the Torrey theory provides a much better fit of the low-temperature T_1 data $(\omega_0^2\tau_c^2\gg1)$ than does the BPP result (14). In this region it is the near neighbors that make the main relaxation contribution, with the remote nuclei providing mainly static terms. The near neighbors are just those for which the distribution of sites deviates most from the BPP assumption of homogeneity, and for which a precise lattice description is most significant.

One advantage of Torrey's method is that it facilitates examination of the $(T_1)_d$ data in the immediate vicinity of the minimum, where the corrections for $(T_1)_e$ are smallest. Substitution of the maximum value of Torrey's b.c.c. Ψ function into (16) results in a prediction of $(T_1)_d=225$ msec at the 9.0-Mc/sec T_1 minimum. The observed value (Fig. 12) is about 190 msec.

In order to examine the dipolar T_2 terms in the data, it is necessary to remove the electron line width contributions. Wangsness and Bloch,[20] in examining the range of validity of the Bloch phenomenological equations,[37] show that in an isotropic medium at high temperatures, where the characteristic frequency of the motion of the

[37] F. Bloch, Phys. Rev. 70, 460 (1946).

TABLE III. Diffusion coefficients in lithium, resulting from interpretation of the relaxation data with an extension of the theory of BPP and with the lattice diffusion theory of H. C. Torrey. E_D is given in kcal/mole and all D_0's are calculated for $E_D = 13.2$ and given in cm²/sec. Indicated average result: $D = (0.24_{-0.10}^{+0.17}) \exp[(-13\,200\pm400)/RT]$ cm²/sec.

ν_0	Region of the data	BPP theory		Torrey theory	
		Relation used	Result	Relation used	Result
9.0 Mc/sec	low temperature $\omega_0^2\tau_c^2\gg1$	T dependence of $(T_1)_d$	$E_D=13.2$	T dependence of $\omega_0\tau$	$E_D=13.2$
		Eq. (14)	$(D_0=0.05)$	Eq. (16), low T asymptote	$D_0=0.30$
	high temperature $\omega_0^2\tau_c^2\ll1$	T dependence of $(T_1)_d$	$E_D=13.0$	Eq. (16), high T asymptote	$D_0=0.20$
		Eq. (15)	$D_0=0.23$		
	T_2' below 370°K	T dependence of T_2'	$E_D=13.2\pm0.4$		
		Eq. (12)	$D_0=0.25$		
3.0 Mc/sec	all $(T_1)_d$ data			T dependence of $\omega_0\tau$	$E_D=13.2$
	at T_1 minimum			$\omega_0\tau/2=0.592$	$D_0=0.26$
15.0, 9.0 6.0, 3.0 Mc/sec	Temperature of T_1 minimum as function of ω_0		$E_D=13$		

magnetic moment is much greater than the Larmor frequency, one has $T_2'=2T_1$. In this case, Eq. (3) becomes $T_2=T_1$, which agrees with a classical argument that at these high frequencies for the nuclear motion the Larmor precession becomes a small effect and T_1 and T_2 represent the same quantity, since the uniqueness of the z-direction is lost. The motions of the conduction electrons are such that $(\omega_c)_e\gg\omega_0$. Therefore, $(T_1)_e=(T_2)_e$ and Eq. (4) becomes, considering only dipolar and conduction electron terms,

$$\left(\frac{1}{T_2'}\right)_d = \frac{1}{T_2} - \left(\frac{1}{2T_1}\right)_d - \left(\frac{1}{T_1}\right)_e. \qquad (17)$$

Turning to the T_2 data, it was found that in Li⁷ near room temperature, where T_1 effects are small, T_2 is independent of the Larmor frequency from 3.0 to 15.0 Mc/sec, as one would expect. In order to inspect the static line width term $(T_2')_d$, we make the reciprocal subtraction described in Eq. (17). We have assumed that any $(T_1)_x$ may be included with the $(T_1)_e$ insofar as line width effects are concerned. The results for the 9.0-Mc/sec data of Fig. 3 are shown in Fig. 14. The line width data of Gutowsky and McGarvey[3] have been converted to T_2' under the assumption of a Lorentz line shape, which is the shape they observed at low temperatures.[38] For this line shape, $T_2=2/(\sqrt{3}\gamma\delta H)$, where δH is measured between the maxima of $d\chi''/dH_0$. The computed T_2's increase from the rigid lattice value and join smoothly onto the low-temperature end of our observations. The data are fitted by an exponential,

corresponding to $E_D=13.2$ kcal/mole, from the lowest temperature at which the narrowing has gotten well under way, up through nearly three decades of T_2'. Beyond 100°C, however, T_2' no longer increases at a constant rate, but rather bends down as if either the activation energy were decreasing [which the $(T_1)_d$ data do not indicate] or another line width interaction were becoming important as the direct dipolar term averages out. The sudden broadening associated with melting is seen to correspond to an order of magnitude decrease in T_2'.

Considering the room-temperature region where T_2' seems to be entirely associated with $(T_2')_d$ and where the T_1 correction is negligible, Eq. (12) and the line drawn in Fig. 14 yield $D=0.25\exp(-13\,200/RT)$ cm²/sec. As has been previously mentioned, the Li⁶ nuclei contribute less than 0.3 percent to $1/T_2'$ and have been neglected here. The results of the dipolar analyses of the Li⁷ data are summarized in Table III. Those data which we have associated with $(T_1)_d$ and $(T_2')_d$ are seen to be in generally good agreement with each other and with the BPP and Torrey theories. As a result of the several independent measurements, we regard the coefficient of self-diffusion for metallic Li⁷ below 400°K as determined to be $D=(0.24_{-0.10}^{+0.17})\exp[(-13\,200\pm400)/RT]$ cm²/sec. The error limits on D_0 are those dictated by the assigned accuracy of E_D. The results in Table III indicate that, within the temperature range of the data, D is determined to ±15 percent. The thermodynamical relation of Nachtrieb et al.[39] gives $E_D=16.5L_m$, where L_m is the latent heat of melting.

[38] H. S. Gutowsky and B. R. McGarvey (private communication).

[39] Nachtrieb, Weil, Catalano, and Lawson, J. Chem. Phys. 20, 1189 (1952).

This appears to work well in many metals, but predicts E_D for lithium to be 11.34 kcal/mole. The earlier Van Liempt relation,[40] $E_D = 32 \times$ melting temperature, predicts 14.5 kcal/mole.

We now consider the T_2 data for both the Li^6 and Li^7 resonances in the enriched Li^6 sample, from Figs. 4 and 5. Although the enriched sample contains 93.8 percent Li^6 and only 6.2 percent Li^7, the Li^7 moments still make an appreciable contribution to the $(T_2')_d$ observed for Li^6. The expression corresponding to Eq. (12) for the case of two nuclear species in the lattice can be shown to be[41]

$$\left(\frac{1}{T_2'}\right)_a = \frac{4\gamma_a{}^4\hbar^2 I_a(I_a+1)N_a}{5Da}$$

$$+ \frac{8\gamma_a{}^2\gamma_b{}^2\hbar^2 I_b(I_b+1)N_b}{15Da}. \quad (18)$$

Figure 15 shows the Li^6 T_2' data corresponding to the data of Fig. 4. The line which passes through the low-temperature points in Fig. 15 is the theoretical result of Eq. (18), if one uses $D = 0.24 \exp(-13\,200/RT)$. The accuracy of the data does not quite permit us to see the 8 percent difference between D for Li^6 and for Li^7 which should arise from the $(m)^{-\frac{1}{2}}$ dependence of D_0. The high-temperature behavior of the Li^6 T_2' is quali-

FIG. 16. T_2' for Na^{23}, calculated from the data of Fig. 6 and plotted against reciprocal temperature. The straight line is a best fit of the data in the region of the exponential dependence of T_2' on temperature.

tatively similar to that observed for Li^7 (Fig. 14) and will be discussed in Sec. IV, C.

The Li^7 resonance in the enriched Li^6 sample gave the results which have been shown in Fig. 5. Again, as for the Li^6, the low-temperature T_2's for the Li^7 are successfully predicted by Eq. (18). There are only vestigial traces of a weak dipolar T_1 minimum in the Li^7 data for this sample, as should be the case because of the weak nuclear dipolar environment.

2. Sodium

The 9.0-Mc/sec sodium data of Fig. 6 have been converted to T_2' by using $1/T_2' = 1/T_2 - 1/T_1$, from Eq. (4). The results are shown in Fig. 16. We have again assumed that any $(T_1)_x$ may be included in $(T_1)_e$ insofar as line-width effects are concerned. As in lithium the relaxation measurements join smoothly onto the T_2' calculated from the line-width data.[2] The exponential section of the data has a slope of 10.0 ± 0.6 kcal/mole. The error here is greater than for the lithium data of Fig. 15 because the exponential region is a decade shorter for the sodium T_2'. Equation (12) and the line drawn in Fig. 16 yield $D = (0.20_{-0.15}{}^{+0.56})$ $\times \exp[(-10\,000 \pm 600)/RT]$, where the limits of error on D_0 correspond to those assigned to E_D. Nachtrieb and co-workers[42] have used the radioactive tracer technique in sodium to measure $D = 0.242 \exp[(-10\,450$
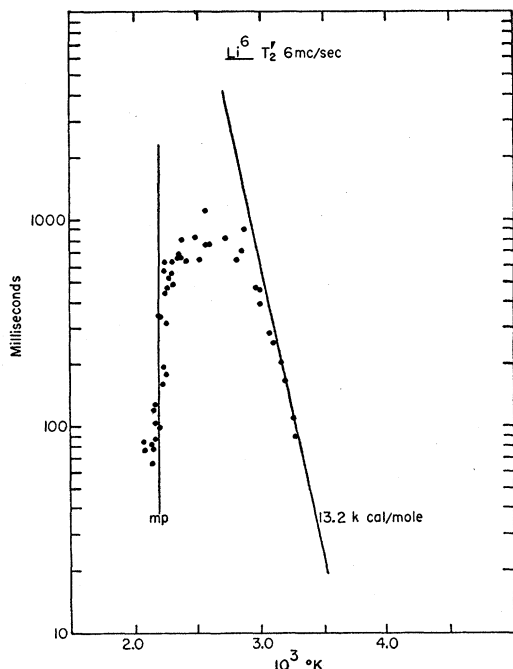

FIG. 15. T_2' for Li^6, calculated from the data of Fig. 4 and plotted against reciprocal temperature. The theoretical line is drawn with the slope determined from the data of Fig. 14 and its position determined by the prediction of Eq. (18).

[40] J. Van Liempt, Z. Phys. 96, 534 (1935).
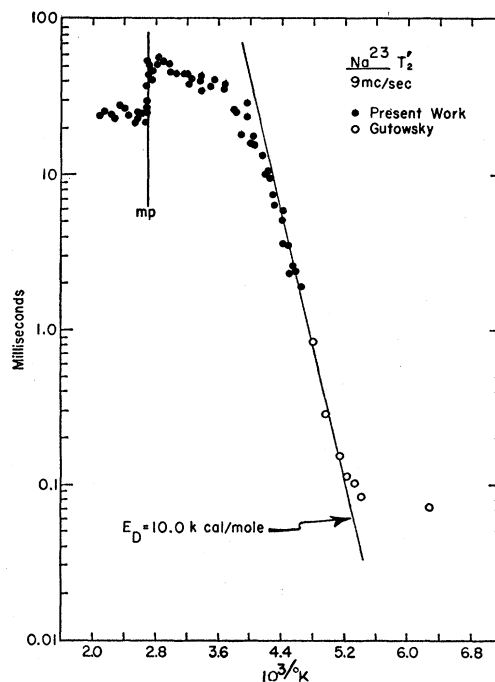[41] D. F. Holcomb, thesis, University of Illinois, 1954 (unpublished).

[42] Nachtrieb, Catalano, and Weil, J. Chem. Phys. 20, 1185 (1952).

$\pm 300)/RT]$ cm²/sec. Thus the nuclear magnetic resonance determination is in agreement with the results of the tracer experiments.

Equation (16), which has been previously shown to describe accurately the $(T_1)_d$ minima observed in Li⁷, predicts $(T_1)_d$ values in sodium of 0.37 and 0.12 sec respectively at the 9- and 3-Mc/sec minima. The temperature of the 3-Mc/sec minimum is calculated to be 265°K from the requirement that $\omega_0\tau_c=0.5922$ at the minimum. The 9-Mc/sec $(T_1)_d$ contribution is completely masked by $(T_1)_e$ (Fig. 10) but, at 3 Mc/sec, a 10 percent dip in T_1 should occur at $10^3/°K=3.77$. The experimental 3-Mc/sec data (Fig. 10) may show this weak minimum.

As in lithium isotopes, T_2' in sodium bends away from the exponential corresponding to Eq. (12) at temperatures well below the melting point and then decreases precipitously at the melting point. Also, as in lithium, the temperature dependence of T_2' in the molten metal is poorly determined, but is certainly small. The high-temperature data will be discussed further in Sec. IV, C.

3. Rubidium

In the rubidium isotopes, we do not have direct T_2 data below the melting point. However, the Rb⁸⁷ line width data reproduced in Fig. 7 and the qualitative similarities to the lithium and sodium data make it fairly certain that in Rb⁸⁷ we have T_1 data which include a diffusion-induced T_1 minimum with $T_2\cong T_1$ on the high-temperature side, and that in Rb⁸⁵ we have just the high-temperature side of a T_1 minimum (and presumably $T_2\cong T_1$). The Rb⁸⁷ minimum at 273°K for 10.5 Mc/sec and the use of $E_D=9$ kcal/mole indicate that the Rb⁸⁵ minimum should occur, for 3.0 Mc/sec, at about 250°K, well below the temperature range of our Rb⁸⁵ measurements. Extending a volume-corrected
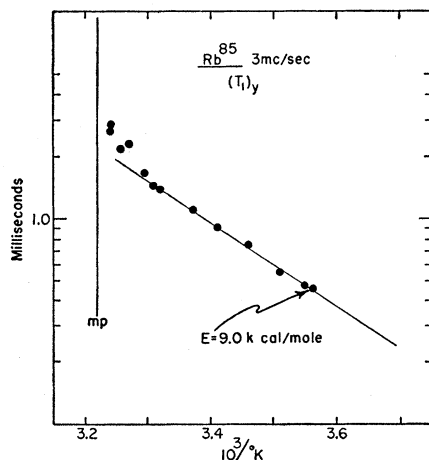

Fig. 17. $(T_1)_y$ for Rb⁸⁵, calculated from the data of Fig. 7 below the melting point by making a correction for $(T_1)_e$. The straight line is the best line through all data except the four points just below the melting point.
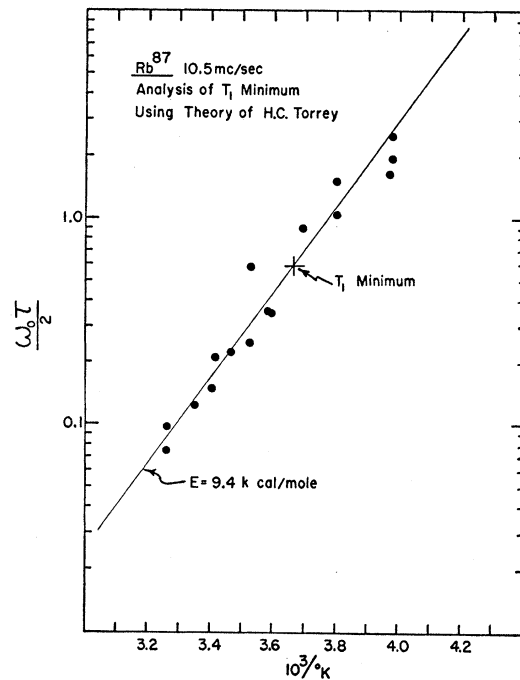

Fig. 18. $(T_1)_y$ for Rb⁸⁷, calculated from the data of Fig. 7 below the melting point by making a correction for $(T_1)_e$. The data have been analyzed using the Torrey theory in the same fashion as the Li⁷ data plotted in Fig. 13.

$(T_1)_e$ from the T_1 data above the melting point, we compute the nonelectron T_1 contribution below the melting point with the expression $1/(T_1)_y=1/T_1 -1/(T_1)_e$. The results for Rb⁸⁵ are shown in Fig. 17. Except for a few points near the melting point (rather large thermal gradients may have existed over the sample which had a volume of several cc), the $(T_1)_y$ fall along a reasonably good exponential with activation energy 9.0 kcal/mole.

Since the Rb⁸⁷ $(T_1)_y$ data correspond only to the immediate region of a T_1 minimum, we have applied the method of Torrey. The results are plotted in Fig. 18 and are seen to be surprisingly exponential in view of the obvious limitation of the experimental accuracy. The slope of the Torrey plot corresponds to $E=9.4$ kcal/mole. The previously mentioned theory of Nachtrieb predicts $E_D=8.6$ kcal/mole for rubidium, while the Van Liempt expression predicts 10.0 kcal/mole.

From the isotopic ratio of $(T_1)_y$'s in the solid, however, it appears that the $(T_1)_y$ mechanism is not entirely the nuclear dipolar interaction. The sample contains 73 percent Rb⁸⁵ and 27 percent Rb⁸⁷. The result of the application of the coupled system T_1 equation analogous to Eq. (18)[41] is that the ratio of $(T_1)_d$ measured in Rb⁸⁵ with respect to that in Rb⁸⁷ is predicted to be 11.2 in the temperature region above the minimum, while the observed ratio near $10^3/°K =3.25$ is about 2. In the next section, we will interpret the T_2 measurements in molten rubidium as indicating

the presence of an additional broadening interaction in Rb[85]. If we regard the small ratio between the T_1's for the isotopes in the solid phase as the result of a similar reduction of T_1 for Rb[85] in the solid, then there is the possibility that the Rb[87] $(T_1)_y$ minimum is entirely dipolar. If so, the Torrey plot (Fig. 18) and Torrey's relation $\omega_0 \tau_c = 0.5922$ at the minimum, yield $D_0 = 0.23$ cm²/sec for $E_D = 9.4$ kcal/mole. This D_0 value is similar to that previously obtained for lithium and sodium.

C. Anomalous Effects, Mainly T_2 at High Temperatures

In this section we consider several aspects of the data which are not clearly understood. The most striking of these effects are the decrease of T_2 at the melting point in lithium and sodium and the line width contribution, in addition to $1/(T_2)_e$ and $1/(T_2)_d$, which is visible in lithium and sodium over a region of about one hundred degrees centigrade below the melting points.

It was first thought that the high-temperature T_2 effects were associated with an interaction of the nuclear quadrupole moment with electric field gradients caused by imperfections in the b.c.c. metallic lattices.[43] In order to check this hypothesis, measurements were made on the Li[6] and Li[7] resonances in the Li[6]-enriched metal obtained from Oak Ridge.[21] For a broadening arising from the postulated quadrupole interaction, there are two possible dependences on the nuclear parameters. If the interaction is subjected to averaging out because of motions in the lattice (as one would expect in the liquid) then[44]

$$1/T_2 \propto Q^2[4I(I+1)-3]/I^2(2I-1)^2.$$

In this case, $(T_2)_{Li^6}/(T_2)_{Li^7} = 507$, since $Q_6/Q_7 = 2.3$

TABLE IV. $(T_2')_x$ in solid and liquid alkali metals near their melting points. The high-temperature static line widths have been calculated in the solids with $(1/T_2')_x = 1/T_2' - (1/T_2')_d$. In the liquids, $(T_2')_x = T_2'$.

	ν_0 (Mc/sec)	H_0 (oe)	Liquid T (°K)	Liquid $(T_2')_x$ msec	Solid T (°K)	Solid $(T_2')_x$ msec
In the Li[6]-enriched sample:						
Li[6]	6	9600	473	81±8	450	480
	3	4800		116±16		
Li[7]	6	3600	473	32±4	450	62
In the samples with natural isotopic abundance:						
Li[7]	15	9100	473	23±3	450	(250)
	9	5400		35±4		220
	6	3600		47±5		
Na[23]	9	8000	390	24±2	313	57
	3	2700		23±3		56
Rb[85]	3	7300	313	7±2		

[43] D. F. Holcomb and R. E. Norberg, Phys. Rev. **93**, 919(A) (1954).

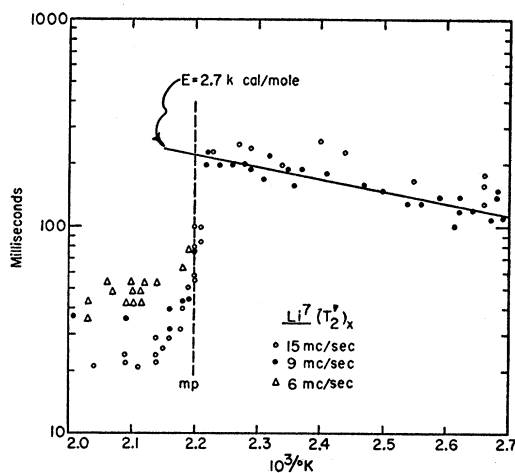[44] R. K. Wangsness and F. Bloch, reference 22, Eq. (5.40).

FIG. 19. The high-temperature contribution to T_2 in Li[7] $(T_2')_x$, which has been calculated by removing the dipolar and conduction electron contributions from the T_2 data measured at several Larmor frequencies.

$\times 10^{-2}$.[45] If, instead, there is some sort of static, un-averaged interaction, one expects

$$1/T_2 \propto Q[4I(I+1)-3]^{\frac{1}{2}}/I(2I-1),$$

in which case $(T_2)_{Li^6}/(T_2)_{Li^7} = 23$. The magnetic moment of Li[6] is also smaller than that of Li[7], but only by a factor of 4, so that magnetic interactions should give rise to smaller T_2 ratios than those given above. As can be seen in Figs. 4 and 5, T_2 above the melting point in Li[6] is less than a factor of 3 longer than T_2 for Li[7] in the same sample. This ratio effectively rules out quadrupolar interactions.

In order to examine the high-temperature line-width term we calculate $(T_2')_x$ from the T_2' data of Sec. IV, B with the appropriate form of Eq. (4); $1/(T_2')_x = 1/T_2' - 1/(T_2')_d$. Table IV lists the results of this manipulation of the data for sodium, rubidium, and the two lithium isotopes. Above the melting points the $(T_2')_d$ correction is negligible and $(T_2')_x$ is just T_2', that is, T_2 with the T_1 contribution removed. It should be noted that the high-temperature broadenings are very small compared to rigid lattice dipolar widths. The T_2 of about 25 msec in molten Li[7] corresponds to a resonance line width of about 0.004 gauss.

The temperature dependence of the $(T_2')_x$ data calculated from the 9.0-Mc/sec Li[7] data of Fig. 14 is shown in Fig. 19. Some data taken at other frequencies are also shown. The absolute values of the $(T_2')_x$ points in the solid lithium are certainly suspect, since they are two correction processes removed from the raw data. The line drawn is a least squares fit of the 9.0-Mc/sec data, arbitrarily assuming an exponential temperature dependence. The individual $(T_2')_x$ data in the liquid are more reliable, since the corrections to T_2 are relatively much smaller than in the solid. The temperature dependence of $(T_2')_x$ in the liquid is small. Although

[45] N. A. Schuster and G. E. Pake, Phys. Rev. **81**, 157 (1951).

the 15.0-Mc/sec data in the solid are in approximate agreement with the 9.0-Mc/sec results, there is a consistent inverse dependence of $(T_2')_x$ in the liquid upon the Larmor frequency.

$(T_2')_x$ obtained from the sodium T_2' data of Fig. 16 shows a temperature dependence in the solid even smaller than that in lithium. Moreover, $(T_2')_x$ drops at the melting point by a factor of only two. The sodium $(T_2')_x$ curves for 9.0 Mc/sec and 3.0 Mc/sec are indistinguishable, with no frequency dependence visible in either the solid or liquid.

The exact mechanisms responsible for the unusual broadenings are not yet understood. However, many of the features of the high-temperature data are consistent with the presence of a magnetic interaction with thermally activated lattice imperfections. We shall list the experimental facts about the broadenings and discuss briefly some of their implications about the nature of the high-temperature interactions.

1. Decrease in T_2 upon Melting

The most striking feature of the data is the sudden decrease in T_2 at the melting point in lithium and sodium. The decrease is unaccompanied by a drop in T_1 other than the previously discussed small variation which arises from the volume dependence of $(T_1)_e$. An interaction is indicated which either appears only upon melting or which becomes much stronger in the liquid.

In some metals the self-diffusion coefficient increases by several orders of magnitude upon melting.[46,47] If this is true in the alkalis, the increased D in the liquid should effectively narrow the nuclear dipolar line width $1/(T_2')_d$ to zero. However, if one assumes that the x-interaction arises from magnetic fields associated with the distorted electron cloud near a vacancy, then, by analogy with (12),

$$1/(T_2')_x \propto n/D_v, \qquad (19)$$

where $n = n_0 \exp(-E_F/RT)$ is the number of vacancies per unit volume. D_v is a diffusion coefficient describing the vacancy motion. If the self-diffusion mechanism is via an atom-vacancy interchange, this D_v is much larger than the atomic self-diffusion coefficient D, and therefore is the determining factor in the narrowing. The activation energy to be associated with D_v is E_M, the barrier or mobility energy. (For the atomic self-diffusion, $E_D = E_F + E_M$.) Thus, (19) becomes

$$(T_2')_x \propto \exp(E_F - E_M/RT). \qquad (20)$$

The effect of melting upon a $(T_2')_x$ described by (19) can be a reduction (that is, a line broadening) if the melting produces a larger increase in n than in D_v.

2. Results in the Solid Metals Near Their Melting Points

The $(T_2')_x$ terms in solid lithium and sodium have several features in common. The data in Table IV

indicate that $(T_2')_x$ in solid lithium and sodium is independent of the Larmor frequency (or of H_0). $(T_2')_x$ first becomes appreciable in lithium and sodium about one hundred degrees centigrade below the melting points (Figs. 14 and 16). This is just the region of temperature in which the resistivities[48] and specific heats[49] become anomalous and where the gradual disintegration of the metallic lattices begins to affect x-ray data.[50] The anomalous resistivity and specific heat terms apparently are associated with the appearance of significant concentrations of thermally activated vacancies in the lattice. Therefore, the explanation of $(T_2')_x$ in this temperature region in terms of a vacancy interaction seems reasonable. However, according to (20), if $E_F > E_M$, which is probably the case, then $(T_2')_x$ should decrease as the temperature rises. Figure 19 shows the opposite to be true. Moreover, crude calculations indicate that a magnetic interaction with the vacancies would not be sufficiently strong to produce the observed effects upon T_2. The situation remains unresolved.

It should be noted that in a solid in which there is vacancy diffusion and in which a vacancy interaction does determine the line width, the temperature dependence indicated by Eq. (20) combined with a knowledge of E_D should permit separate determination of E_F and E_M. Bloembergen[51] has independently recognized this fact.

The unexplained ratios of the T_1's measured in the solid for the two rubidium isotopes (Sec. IV, B) may be connected with the interactions which cause the $(T_2')_x$ effects in all three alkalis, but the point is not clear.

3. Results in the Liquid Metals

$(T_2')_x$ in liquid lithium is independent of the isotopic species of the surrounding nuclei (Table IV). The high-temperature T_2 in Fig. 3 for Li^7 in a sample of natural isotopic abundance is approximately the same as T_2 in Fig. 5 for Li^7 in the 93 percent Li^6 sample. Since the local fields caused by the nuclear moments are very different in the two samples, the source of the local fields responsible for the reduced T_2 in the liquid must be external to the nuclear spin system. The similarity of the T_2's in the liquids is surprising in view of the nonequality of the T_2's in the solid samples. In Sec. 4, below, we describe evidence for impurity effects on T_2 in lithium which are important below the melting point but are not evident in the liquid.

$(T_2')_x$ in liquid lithium and sodium is nearly temperature independent. Bloembergen and Rowland[8] have observed the resonance lines in two liquid Hg-Tl alloys to be insensitive to temperat ureand not appreciably narrower than in the solid phases. The $(T_2')_x$ interaction

[46] W. Jost, *Diffusion in Solids, Liquids, Gases* (Academic Press, Inc., New York, 1952), p. 335.
[47] Careri, Paoletti, and Salvetti, Nuovo cimento 11, 399 (1954).

[48] D. K. C. MacDonald, J. Chem. Phys. 21, 177 (1953).
[49] L. G. Carpenter, J. Chem. Phys. 21, 2244 (1953).
[50] C. C. Bidwell, Phys. Rev. 27, 381 (1926).
[51] N. Bloembergen (to be published).

present in the molten alkalis may be a feature common to many liquid metals and alloys.

From the data presented here and the measurements of Bloembergen and Rowland, it appears that many liquid metals may have T_2 values appreciably less than T_1. Such is not the case for those nonmetallic liquids upon which measurements have been reported. The conduction electrons appear to be the source of the magnetic local fields which determine the line widths in those liquid metals which exhibit T_2 values not determined by T_1. The line widths in liquid lithium and sodium may be the result of anomalous local fields arising from distortion of the electron distribution in the vicinity of imperfections. Since no unusual behavior of T_1 is observed near the melting points, the local magnetic fields in question presumably result from a polarization effect and lie only along the direction of H_0. The alternate explanation for the lack of a T_1 effect would be a low-correlation frequency for the high-temperature interaction, which seems quite unlikely in the liquid metals.

4. Dependence of the Results upon the Purity of the Samples

The indications that the high-temperature broadenings arise from interaction with magnetic field sources external to the nuclear spin system lead one to suspect impurities in the metals as a source of some of the anomalous effects. Unfortunately, the total impurity content of our samples is not well known. We do know the metallic impurities in the lithium and sodium samples from spectrographic analyses (Table I). There appears to be little dependence of the data upon these impurities. Lithium samples A and B have sodium as their primary impurity, and differ by a factor of 10 in their sodium contents. Yet the data in Fig. 3 show no difference between the T_2's shown as dots, which were obtained using sample A and those indicated by triangles, which were measured in sample B. It appears more likely that the impurities significant for T_2 might be chemical compounds on the surface or dissolved into the metal particles. Because of the high chemical reactivity of the alkali metals, it is difficult to prevent the occurrence of chemical reactions on the surfaces of the metal particles. There is some evidence that non-metallic impurities can play a role in the extra broad-

enings, at least in the region just below the melting points. A comparison of Figs. 3 and 5 shows that, as has been mentioned in Part 3, there are definitely smaller T_2's below the melting point in Fig. 5. A similar reduction of T_2 in the region just below the melting point was produced in lithium sample A by removing most of the oil from the sample (in air) so that there was no protective coating on the particle surfaces. Fortunately, we do have good evidence that at least the major part of the extra broadenings is independent of the surface condition. Dr. T. R. Carver was able to produce, under a helium atmosphere and in a degassed oil, a lithium dispersion in which the particles retained a bright metallic sheen. The T_2 measurements given as triangles in Fig. 3 were made with this sample. They agree with the other T_2 measurements in Fig. 3 which were made in a sample in which the particles were visibly darkened, probably because of the formation of lithium azide at the surfaces.

No differences in T_2 among the various samples was observed above the melting point.

The sodium sample listed as B in Table I gave T_2's lower than those given in Fig. 6. In B, lower T_2's were also observed above the melting point. A small extra decrease of T_1 was observed in the liquid, although T_1 in the solid agrees with the data in Fig. 6. This is the only sample in any of the metals in which a sample dependence of T_1 was observed.

Quantitative investigation of the anomalous effects considered in Sec. IV, particularly in the solid phase in the temperature region just below the melting point, evidently requires more careful control of sample purity than has been achieved in this work.